Supplementary material for

Diagnostic Classification for Human Autism and Obsessive-Compulsive Disorder Based on Machine Learning From a Primate Genetic Model

Yafeng Zhan, M.S., Jianze Wei, M.S., Jian Liang, Ph.D., Xiu Xu, M.D., Ran He, Ph.D.,

Trevor W. Robbins, Ph.D., Zheng Wang, Ph.D.

*Correspondence: zheng.wang@ion.ac.cn (Z. W.); rhe@nlpr.ia.ac.cn (R. H.)

This PDF file includes:

Materials and Methods

Supplementary References

Figure S1 to S5

Table S1-S10

Materials and Methods

Animal preparation

All experimental procedures for nonhuman primate research in this study were approved by the Institutional Animal Care and Use Committee in the Institute of Neuroscience and by the Biomedical Research Ethics Committee, Shanghai Institutes for Biological Sciences, Chinese Academy of Sciences, and conformed to National Institutes of Health guidelines for the humane care and use of laboratory animals.

The monkey dataset included five *MECP2*-duplication transgenic (TG) monkeys (*Macaca fascicularis*, aged 4.40 ± 0.29 years (mean ± SD), weight 3.26 ± 0.75 kg; 2 male, 3 female) and 11 wild-type (WT) monkeys (*Macaca fascicularis*, aged 4.68 ± 0.46 years, weight 3.97 ± 1.36 kg; 4 male, 7 female). All 16 monkeys were prepared and maintained in a stable brain state for fMRI scans. The fMRI scanning process for all monkeys was conducted in a similar manner to our previous work (1, 2). Before each scanning session, anesthesia of the animals was inducted with an intramuscular injection of ketamine (10 mg per kg) and atropine sulfate (0.05 mg per kg). After intubation, animals were ventilated with an MRI-compatible ventilator (CWE Inc., Weston, Wisconsin). Macaques were maintained with intermittent positive-pressure ventilation to ensure a constant respiration rate (25-35 breaths/min). Local anesthetic (5% lidocaine cream) was applied around the ears to block peripheral nerve stimulation. The monkeys were then placed in a custom-built MRI-compatible stereotaxic frame with their belly facing downward, and their heads were secured before being inserted into the center of AC88 bores.

In light of the anesthesiologist's instructions, anesthesia was maintained using the lowest possible concentration of isoflurane gas. Isoflurane was selected for the scans as resting-state networks have previously been demonstrated to be present while using this agent (1, 3-5). The vital signs of animals including blood oxygenation, ECG, rectal temperature (Small Animal Instruments, Inc., Stony Brook, New York), respiration rate and end-tidal CO_2 (Smiths Medical ASD Inc., Dublin, Ohio) were continuously monitored throughout the duration of the experiment. Oxygen saturation was kept at over 95% and body temperature was kept constant using a hot water blanket (Gaymar Industries Inc., Orchard Park, New York). Lactated Ringer's solution was given with a maximum rate of 10 ml/kg/hour during the anesthesia process (6). Note that our intention was to equate the levels of physiological anesthesia across animals and not the level of anesthetic gas concentration. Slight individual differences in physiology meant that slight differences in anesthetic gas concentrations were needed to impose a similar level of anesthesia on different monkeys (7). Brain states were monitored by simultaneous MRI-compatible electroencephalograph (EEG) (Brain Products GmbH, Gilching, Germany) during data acquisition. Within the range of isoflurane levels used in the current study, consistent patterns of functional coupling between distant brain areas have been reported in prior monkey fMRI studies (5, 8) and demonstrated in our work as well (1, 2).

Human Participants

Human ASD cohort. We analyzed data from the ABIDE-I/II repository (9, 10) and an ADHD cohort from ADHD-200 (11), two publicly available multisite datasets of resting-state functional imaging data, and one OCD cohort from our institutional database. The ABIDE initiative now includes two large-scale collections: ABIDE-I and ABIDE-II. Each collection was created through the aggregation of datasets independently collected across more than 17 international brain imaging laboratories (9, 10). In the present study, two cohorts of human ASD data were selected from ABIDE-I and ABIDE-II separately. We included all individuals with a diagnosis of either autism, Asperger syndrome, or pervasive developmental disorder not otherwise specified (PDD-NOS), collectively referred to as the ASD group according to the Diagnostic and Statistical Manual of Mental Disorders, Fourth Edition, Text Revision (*DSM-IV-TR)*, as well as demographically matched healthy control (HC) subjects. As with other ABIDE studies (10, 12), participant inclusion criteria were as follows: (1) right-handedness; (2) a full-scale IQ (FIQ) score higher than 80; (3) ASD individuals with known current medication status; (4) a mean framewise displacement (FD) (13) of less than 0.2mm and the percent of frames or volumes with displacement greater than 0.2mm < 50%; (5) individuals with known eye status at scan (open/closed); (6) data with anatomical images providing near full brain coverage and successful registration; and (7) sites with at least 5 participants per group and matched number of participants between two groups after applying these inclusion criteria. This yielded data for 336 individuals (ASD = 133, male/female = 118/15, mean±SD age = 17.25±7.76 years; HCs = 203, male/female = 167/36, mean±SD age = 16.66±6.33 years) from 10 sites for ABIDE-I and 149 individuals (ASD = 60, male/female = 56/4, mean±SD age = 11.95±4.33 years; HCs = 89, male/female = 62/27, mean±SD age = 11.40±3.59 years) from 4 sites for ABIDE-II. More details of ASD samples are specified in Table S2 and S3.

Human ADHD cohort. The open-access, freely accessible Attention Deficit and Hyperactivity Disorder (ADHD-200 Sample) database (http://fcon_1000.projects.nitrc.org/indi/adhd200/) was used to obtain datasets with resting-state data of individuals with ADHD and healthy controls. In the present study, the inclusion criteria included: (1) right-handedness; (2) an FIQ score higher than 80; (3) ADHD individuals with known current medication status; (4) individuals with images accepted after quality control. Individuals with translation or rotation in any axis of head motion larger than 3mm or 3° during scanning were excluded after applying the above inclusion criteria. These criteria led to the inclusion of data from the Kennedy Krieger Institute ("KKI"), Oregon Health & Science University ("OHSU") and Peking ("Peking") study-sites. Note that, for sites that contributed several functional runs per participant (OHSU), we only used the first functional run in the present study. Sites with less than 5 participants per group and a mismatched number of participants between two groups after the above criteria applied were excluded. We selected ADHD participants with known current medication status and with images accepted after quality control. This yielded data for 275 individuals (ADHD = 102, male/female = 85/17, mean±SD = 11.57±2.23 years; HCs = 173, male/female = 99/74, mean±SD age= 10.96±1.81 years) for ADHD. More details of ADHD samples are specified in Table S4.

Human OCD cohort. Between April 2013 and September 2016, patients were recruited through local inpatient and outpatient departments at the OCD Clinics at Ruijin Hospital. All participants provided written informed consent for study participation after receiving a complete description of the protocols, which were approved by the Institutional Review Boards at Ruijin Hospital, Shanghai Jiao Tong University and by the Biomedical Research Ethics Committee, Shanghai Institutes for Biological Sciences, and Chinese Academy of Sciences. All patients had received a primary diagnosis of OCD based on clinical evaluation with the Chinese translation of the Structured Clinical Interview for *DSM-IV-TR*, and were administered the Yale-Brown Obsessive Compulsive Scale (Y-BOCS) (14) and Hamilton Anxiety Scale (HAM-A) to assess OCD symptom severity. Exclusion criteria were applied as follows: (1) translation or rotation in any axis of head motion larger than 3mm or 3° during scanning; (2) any neurological disorders, psychosurgery, current or past substance abuse or dependence, pregnancy or any substantial physical illness such as brain tumor, brain injury, stroke, or epilepsy. The OCD dataset consisted of 171 individuals (OCD = 92, male/female = 55/37, mean±SD age = 30.47±9.30 years; HCs = 79, male/female = 51/28, mean±SD age = 30.80±7.77 years). More details of OCD samples are specified in Table S5.

Monkey MRI data acquisition and preprocessing

MRI images of all monkeys were acquired at the Institute of Neuroscience on a 3T whole-body scanner (Trio; Siemens Healthcare, Erlangen, Germany) running with an enhanced gradient coil insert (AC88; 80 mT/m maximum gradient strength, 800 mT/m/s maximum slew rate). A custom-built 8-channel phased-array transceiver coil was used for animal imaging sessions. Whole-brain resting-state fMRI data were collected using a gradient-echo echo-planar sequence (repetition time [TR] = 2000 ms; echo time [TE] = 29 ms; flip angle = 77°; slices = 32; matrix = 64 × 64; field of view = 96 × 96 mm; 1.5 × 1.5 mm^2 in plane resolution; slice thickness = 2.5 mm; GRAPPA factor = 2). For each session, 5 to 10 runs were acquired and each run consisted of 200 functional volumes. A pair of gradient echo images (TE: 4.22 ms and 6.68 ms) with the same orientation and resolution as EPI images were acquired to generate a field map for distortion correction of EPI images. High-resolution T1-weighted anatomical images were acquired using a MPRAGE sequence (TR = 2500 ms; TE = 3.12 ms; inversion time = 1100 ms; flip angle = 9°; acquisition voxel size = 0.5 × 0.5 × 0.5 mm^3; 144 sagittal slices). Six whole-brain anatomical volumes were acquired and further averaged for better brain segmentation and 3D cortical reconstruction. In the present experimental design, we did not intentionally collect different numbers of runs from each subject. In practice, however, the actual scan time for each experiment varied with the physiological status of different animals on that day, as is the case in most animal fMRI studies (5, 8, 15). In the final analysis, we included a total of 45 runs from TG and 99 runs from WT monkeys. Details of run numbers and physiological parameters for each animal are listed in Table S1.

Functional images of monkey and human brains were preprocessed using exactly the same strategy, which included slice timing correction, motion correction, coregistration with individual T1-weighted image, normalization to corresponding standard space, reslicing and spatial smoothing, regression of nuisance signals, removal of linear drift and temporal filtering (0.01 - 0.1 Hz). Specifically, the preprocessing of the monkey data were done using the SPM 8.0 toolbox (http://www.fil.ion.ucl.ac.uk/spm) and the FMRIB Software Library toolbox (FSL; https://fsl.fmrib.ox.ac.uk/fsl). The first 10 volumes were discarded. The field map images of each participant were then applied to compensate for the geometric distortion of EPI images caused by magnetic field inhomogeneity using FSL FUGUE. After slice timing correction and motion correction, the corrected images were normalized to standard space of the monkey F99 atlas (http://sumsdb.wustl.edu/sums/macaque_more.do) using an optimum 12-parameter affine transformation and nonlinear deformations, and then resampled to 2-mm cubic voxels and spatially smoothed with a 4 mm full-width at half-maximum (FWHM) isotropic Gaussian kernel. Six head motion parameters, ventricle and white matter signals were removed from the smoothed volumes using linear regression. Linear drift of the volumes was removed and a temporal filter was performed.

Human MRI data acquisition and preprocessing

Details available for ABIDE-I/II at http://fcon_1000.projects.nitrc.org/indi/abide/ and ADHD-200 at http://fcon_1000.projects.nitrc.org/indi/adhd200/. The imaging parameters of ASD and ADHD cohorts are listed in Table S6. OCD MRI data were collected using a Siemens Tim Trio 3T scanner (Erlangen, Germany). All participants underwent both functional and structural MRI scanning. Resting-state fMRI scans of the whole brain were acquired using a T2*-weighted EPI (echo planar imaging) sequence: repetition time (TR) = 3000 ms; echo time (TE) = 30 ms; flip angle, 90°; 47 axial slices; 3 mm slice thickness with no gap; and 300 volumes. High-resolution T1-weighted images used a magnetization prepared rapid gradient echo sequence: TR = 2300 ms; TE = 3 ms; inversion time, 1000 ms; flip angle, 9°;1×1×1 mm^3 spatial resolution. During the resting-state scan, participants were instructed to stay awake but relaxed, with their eyes closed, remain motionless, and refrain from thinking about anything in particular.

ASD and ADHD data preprocessing. The preprocessing of ABIDE-I was performed by the Preprocessed Connectomes Project (PCP, http://preprocessed-connectomes-project.org/abide/index.html) using the Data Processing Assistant for Resting-State fMRI (DPARSF) Toolbox (16). Preprocessing steps included slice timing correction, motion correction, spatial normalization into MNI space, reslicing to 3 × 3 × 3 mm voxels and smoothing with a Gaussian kernel (FWHM = 6 mm). Friston-24 parameters of head motion, white matter and ventricle signals were regressed out, followed by linear drift correction and temporal filtering (0.01 - 0.1 Hz). For more details, readers are suggested to refer to the description in the PCP (http://preprocessed-connectomes-project.org/abide/dparsf.html). The same preprocessing streamline was applied to the ABIDE-II and

ADHD data sets using DPARSF Toolbox.

OCD data preprocessing. Preprocessing for OCD data were the same as the ABIDE PCP pipeline using DPARSF Toolbox except for minimal differences in some parameters, a smaller smoothing kernel (i.e. 2 mm), six head-motion parameters were regressed, and temporal filtering was applied (0.01 - 0.08HZ) for OCD.

Sparse linear regression model based on group lasso method

We adopted the sparse linear regression model based on group lasso method penalty (17) to identify a subset of core brain regions relevant to ASD from *MECP2* monkeys.

Let $\{(A^{(1)},\ Y_1), \dots, (A^{(M)},\ Y_M)\}$ be the M monkey sample of undirected adjacency matrices with N nodes and with their class labels y. The adjacency matrices A of each sample were reshaped into a one-dimensional vector and stacked, forming a feature matrix $B \in \mathbb{R}^{M\times P}$ (M samples and P features, $P = N \times (N-1)$). Let $y = (Y_1, \dots, Y_M)$ denotes the M dimensional response vector (e.g. the diagnostic label, that is $y = 1$ indicates TG and $y = 0$ indicates WT class). The sparse linear regression model based on group lasso penalty can then be formulated as

$$\min_{x\in\mathbb{R}^P} F(x) = \frac{1}{2}\left\| y - \sum_{n=1}^{N} [B]_n [x]_n \right\|_2^2 + \lambda \sum_{n=1}^{N} w_n \|[x]_n\|_2 \qquad (1)$$

where λ is a positive regularization parameter with 100 equally spaced points between 0.05 and 1. In this setting, the original feature matrix B was partitioned into N groups (treating all edges connected to one node as a group) $[B]_1, [B]_2, \dots\dots, [B]_N$ and w_n denotes the weight for the n-th group. Note that, here we used screening rule proposed by Wang, Wonka (18) to solve group lasso efficiently. After solving the group lasso problem, we obtained the corresponding N solution vector $[x]_1, [x]_2, \ldots \ldots, [x]_N$ and the dimension of $[x]_n$ is the same as the feature space in $[B]_n$. The relevant group features selected at each regularization parameter were combined by the union operation, to avoid the tweaking of such parameters.

Cross-species diagnostic classification for human individuals

The group lasso algorithm automatically and objectively identified 9 core regions from transgenic monkeys. The monkey sample (both transgenic and wild-type groups were under same anesthesia) was used solely for the extraction of core regions. We subsequently made a one-to-one mapping of the identified core regions to the human brain network to pre-selecting all edges that connected to the regions from in human correlation matrix, comprising 801 unique FCs. The final classifier was built on the human data and the actual classification was carried out in multiple, independent, large-scale human datasets. Specifically, the procedure for selecting relevant FCs from the pre-selected FCs (801 FCs), training a predictive model, and assessing its generalization ability was carried out as a sequential process of 10×10 nested feature-selection (FS) and leave-one-out cross-validation (Figure S1). The details are shown below.

The whole data set was stratified into ten folds: one was left out as the testing pool for LOOCV, and the remaining 9 folds (outer loop training data) were used for constructing the optimal features.

Inner feature selection loop:

The outer loop training data was stratified into ten folds: one was left out, and the remaining 9 folds (inner loop training data) were subject to lasso feature selection (19). . Optimal features were the union of the functional connections (FCs) selected throughout the inner loop.

Outer LOOCV predicting loop:

In each LOOCV fold, one sample was taken from the testing pool of the outer loop and used as a test set for evaluation. The remaining samples were used to train a SLR classifier on optimal features retained during the inner training loop. This procedure is repeated for every sample in the testing pool of the outer loop.

The feature (FCs) selection procedure was similar to 10×10 nested cross-validation, with the difference that the test set was never used for validation or feature (FCs) selection. In this way, the lasso was trained on different subsamples of the data set, to increase the stability of the selected features. The 'test set' of the outer loop FS process was kept as a testing pool for LOOCV, whereas the ten folds of the inner loop FS were used to select features. Consequently, the LOOCV folds that belonged to the same testing pool of the outer loop FS shared the same reduced features. In the inner loop FS, the FS was completed using MATLAB's *Statistics and regression Toolbox* (Mathworks Inc.). FCs were selected using the default setting of the *lasso* function. The hyperparameter λ was estimated default by *lasso*. The features selected at each inner fold and λ were combined by the union operation, to include features that are important for any possible subsample (inner ten folds) of the training data set. Once the inner loop FS was executed, one sample was taken from the testing pool of the outer loop FS, and used as the test set of the LOOCV. The remaining samples were used to train SLR on the FCs retained during the inner loop FS (as illustrated in Figure S1).

Sparse logistic regression classifier

To predict the diagnostic label from the extracted features (optimal FCs, z), we employed logistic regression as the classifier. In logistic regression, a logistic function is used to define the probability of a participant belonging to the ASD class as

$$P(y = 1 \mid \hat{z}; w) = \frac{1}{1 + \exp(-w^T \hat{z})} \qquad (2)$$

where y represents the diagnosis class label, that is $y = 1$ indicates ASD and $y = 0$ indicates HC class, respectively. $\hat{z} = [z^T, 1]^T \in \mathbb{R}^{k+1}$ is a feature vector with an augmented input. $w \in \mathbb{R}^{k+1}$ is the weight vector of the logistic function. SLR automatically selects the features related to the ASD label as input for the logistic function. In SLR, the probability distribution of the parameter vector is estimated using the hierarchical Bayesian estimation approach, in which the prior distribution of each element of the parameter vector is represented as a Gaussian distribution. Because of the automatic relevance determination property of the hierarchical Bayesian estimation method, some of the Gaussian distributions become sharply peaked at zero so that the irrelevant features are not used in the classification (20).

Model Validation and Comparison

To test model robustness, a non-parametric permutation test was performed to determine whether the classification accuracy was due to chance. The entire classification analysis was repeated 5,000 times with random shuffling of the human group labels using the set of 9 core regions identified from the monkey cohort. This procedure estimated the null distribution of classification accuracy, and the significant p value was estimated by identifying the proportion of the total number for which the classification accuracy was greater than that of the observed one. Moreover, the reliability of the proposed cross-species translational framework was further tested under conditions where 9 core regions were randomly selected from the 94 regions to evaluate whether the probability of getting accuracy values was significantly higher than chance level (n = 5,000 iterations). For model comparison, we compared the predictive accuracies of two classification models, i.e. the monkey-derived classifier and the human-derived classifier, using McNemar's test (21). Specifically, the monkey-derived classifier was constructed based on core regions identified from monkey data, the human-derived classifier was constructed based on core regions identified from human ASD cohort.

References

1. Wang Z, Chen LM, Negyessy L, et al.: The relationship of anatomical and functional connectivity to resting-state connectivity in primate somatosensory cortex. Neuron 2013; 78:1116-1126.
2. Lv Q, Yang L, Li G, et al.: Large-Scale Persistent Network Reconfiguration Induced by Ketamine in Anesthetized Monkeys: Relevance to Mood Disorders. Biol Psychiatry 2016; 79:765-775.
3. Shen K, Bezgin G, Hutchison RM, et al.: Information processing architecture of functionally defined clusters in the macaque cortex. J Neurosci 2012; 32:17465-17476.
4. Hutchison RM, Womelsdorf T, Gati JS, et al.: Resting-state networks show dynamic functional connectivity in awake humans and anesthetized macaques. Hum Brain Mapp 2013; 34:2154-2177.
5. Vincent JL, Patel GH, Fox MD, et al.: Intrinsic functional architecture in the anaesthetized monkey brain. Nature 2007; 447:83-86.
6. Logothetis NK, Guggenberger H, Peled S, et al.: Functional imaging of the monkey brain. Nat Neurosci 1999; 2:555-562.
7. Sallet J, Mars RB, Noonan MP, et al.: The organization of dorsal frontal cortex in humans and macaques. J Neurosci 2013; 33:12255-12274.
8. Hutchison RM, Hutchison M, Manning KY, et al.: Isoflurane induces dose-dependent alterations in the cortical connectivity profiles and dynamic properties of the brain's functional architecture. Hum Brain Mapp 2014; 35:5754-5775.
9. Di Martino A, O'Connor D, Chen B, et al.: Enhancing studies of the connectome in autism using the autism brain imaging data exchange II. Sci Data 2017; 4:170010.
10. Di Martino A, Yan CG, Li Q, et al.: The autism brain imaging data exchange: towards a large-scale evaluation of the intrinsic brain architecture in autism. Mol Psychiatry 2014; 19:659-667.
11. Consortium HD: The ADHD-200 Consortium: A Model to Advance the Translational Potential of Neuroimaging in Clinical Neuroscience. Front Syst Neurosci 2012; 6:62.
12. Catani M, Dell'Acqua F, Budisavljevic S, et al.: Frontal networks in adults with autism spectrum disorder. Brain 2016; 139:616-630.
13. Power JD, Barnes KA, Snyder AZ, et al.: Spurious but systematic correlations in functional connectivity MRI networks arise from subject motion. Neuroimage 2012; 59:2142-2154.
14. Goodman WK, Price LH, Rasmussen SA, et al.: The Yale-Brown Obsessive Compulsive Scale. I. Development, use, and reliability. Arch Gen Psychiatry 1989; 46:1006-1011.
15. Hutchison RM, Everling S: Monkey in the middle: why non-human primates are needed to bridge the gap in resting-state investigations. Front Neuroanat 2012; 6:29.
16. Chao-Gan Y, Yu-Feng Z: DPARSF: A MATLAB Toolbox for "Pipeline" Data Analysis of Resting-State fMRI. Front Syst Neurosci 2010; 4:13.
17. Yuan M, Lin Y: Model selection and estimation in regression with grouped variables. J Roy Stat Soc B 2006; 68:49-67.
18. Wang J, Wonka P, Ye JP: Lasso screening rules via dual polytope projection. J Mach Learn Res 2015; 16:1063-1101.
19. Tibshirani R: Regression shrinkage and selection via the Lasso. J Roy Stat Soc B Met 1996; 58:267-288.
20. Yamashita O, Sato MA, Yoshioka T, et al.: Sparse estimation automatically selects voxels relevant

for the decoding of fMRI activity patterns. Neuroimage 2008; 42:1414-1429.
21. McNemar Q: Note on the Sampling Error of the Difference between Correlated Proportions or Percentages. Psychometrika 1947; 12:153-157.

Supplementary Figures

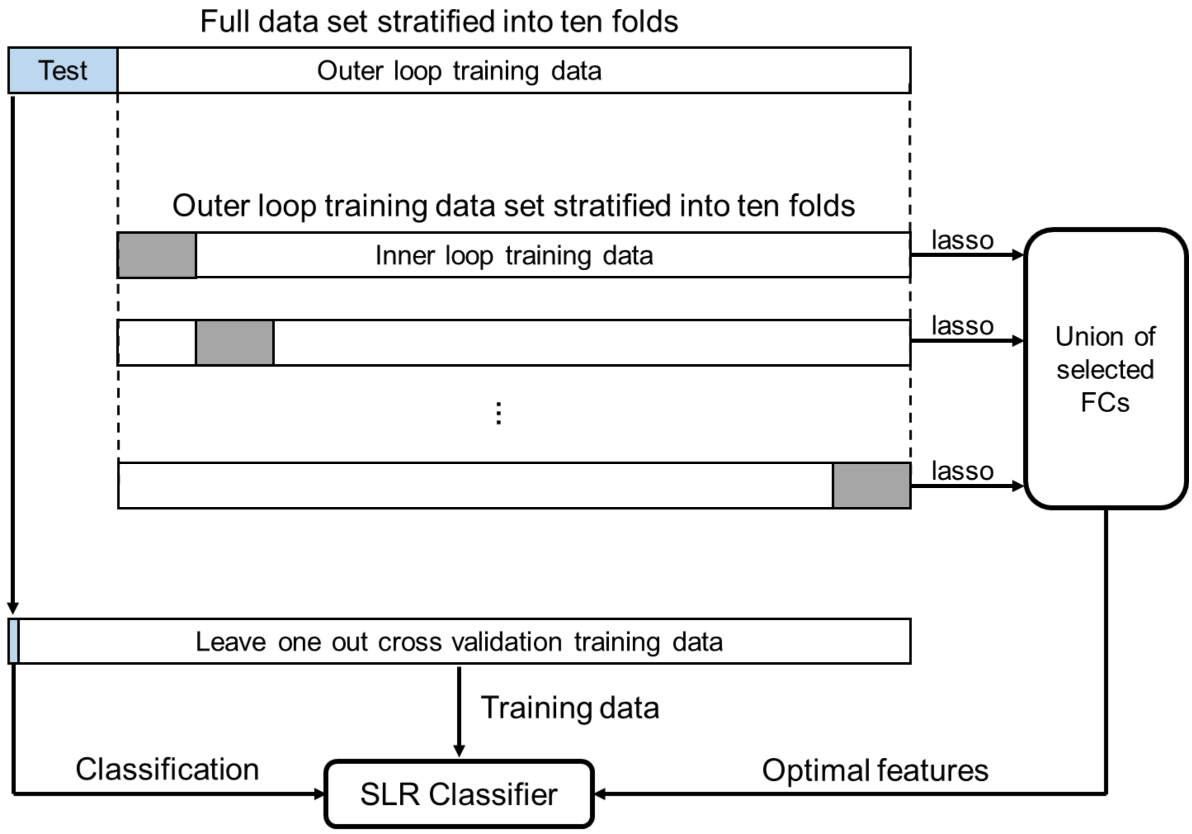

Figure S1. Illustration of nested 10×10 feature selection and leave-one-out cross-validation.

I. The full data set was stratified into ten folds: one was left out as the testing pool for LOOCV, and the remaining 9 folds (outer loop training data) were used for constructing the optimal features.

II. In the inner loop, the outer loop training data was stratified into ten folds, one was first left out, and the remaining 9 folds (inner loop training data) were subjected to lasso feature selection. Optimal features were the union of the functional connections (FCs) selected throughout the inner loop.

III. In each LOOCV fold, one sample was taken from the testing pool of the outer loop and used as test set for LOOCV evaluation. The remaining samples are used to train SLR on optimal features retained during the inner loop. This procedure is repeated for every sample in the testing pool of the outer loop.

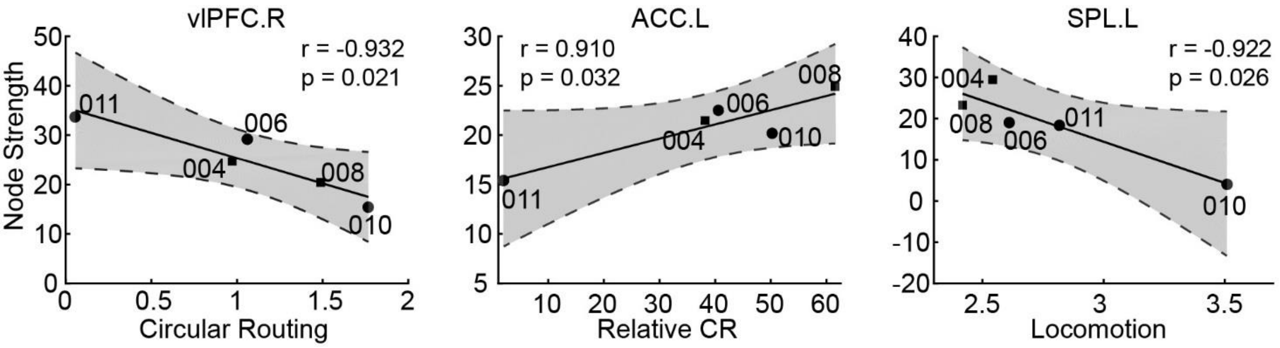

Figure S2. Correlation between node strength of core regions and behavior abnormalities in TG group.

A circle shape denotes female and a square shape denotes male, with labels indicating monkey ID. Gray zone indicates a 95% confidence interval. vlPFC.R, right ventrolateral prefrontal cortex; ACC.L, left anterior cingulate cortex; SPL.L, left superior parietal cortex; CR, circular routing.

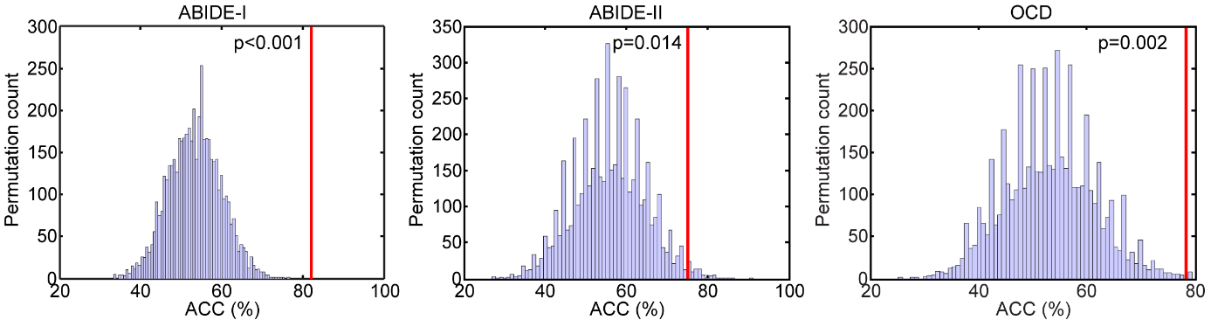

Figure S3. Null distribution of classification accuracy in the permutation test.

The histograms of the permutation test (5,000 repetitions) for ASD (ABIDE-I and ABIDE-II) and OCD data. The purple bars represent the number of permutation counts at each level of accuracy. The vertical red lines denote the observed accuracies, corresponding to a p-value of $p<0.001$ for ABIDE-I, $p=0.014$ for ABIDE-II, and $p=0.002$ for OCD.

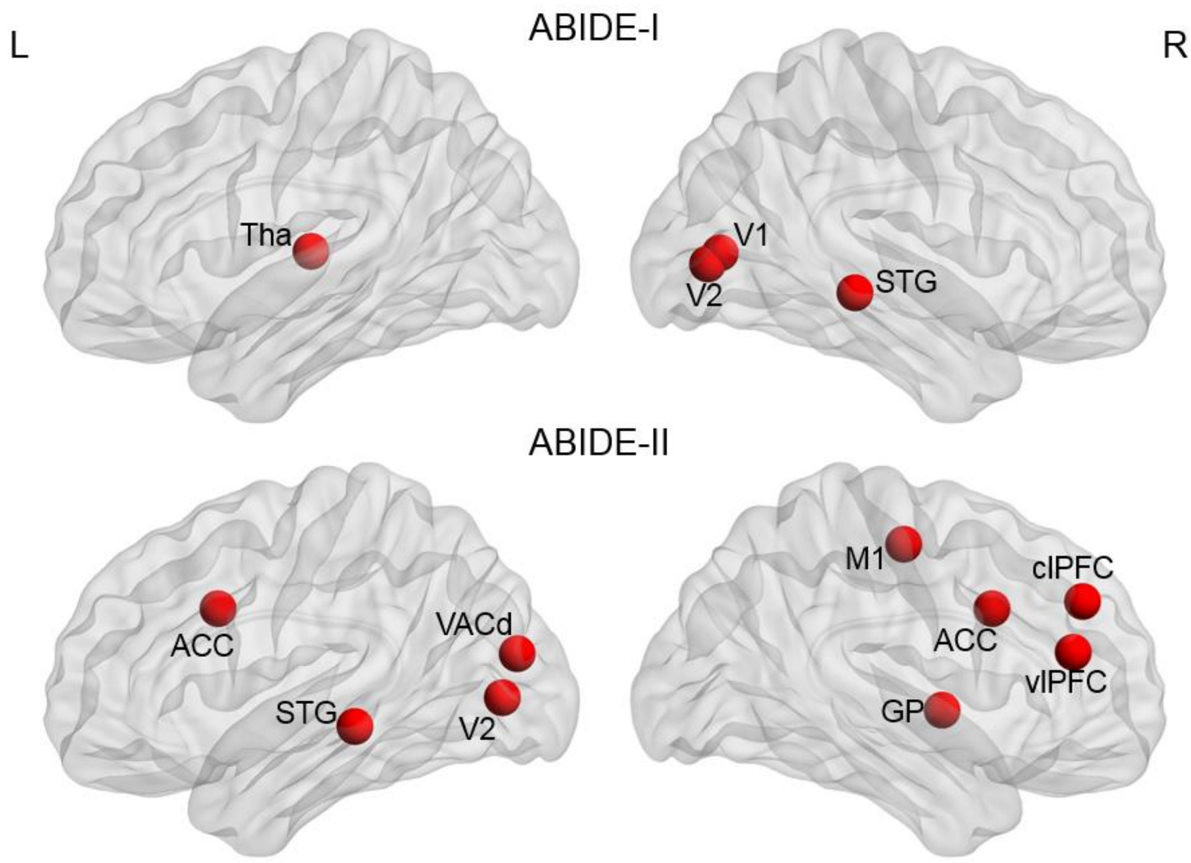

Figure S4. Identified core regions using ABIDE-I and ABIDE-II datasets.

Core regions identified by group lasso in ABIDE-I and ABIDE-II cohorts. Tha, thalamus; V1, primary visual cortex; V2, secondary visual cortex; STG, superior temporal cortex; ACC, anterior cingulate cortex; VACd, dorsal part of the anterior visual area; M1, primary motor cortex; GP, globus pallidus; clPFC, centrolateral prefrontal cortex; vlPFC, ventrolateral prefrontal cortex.

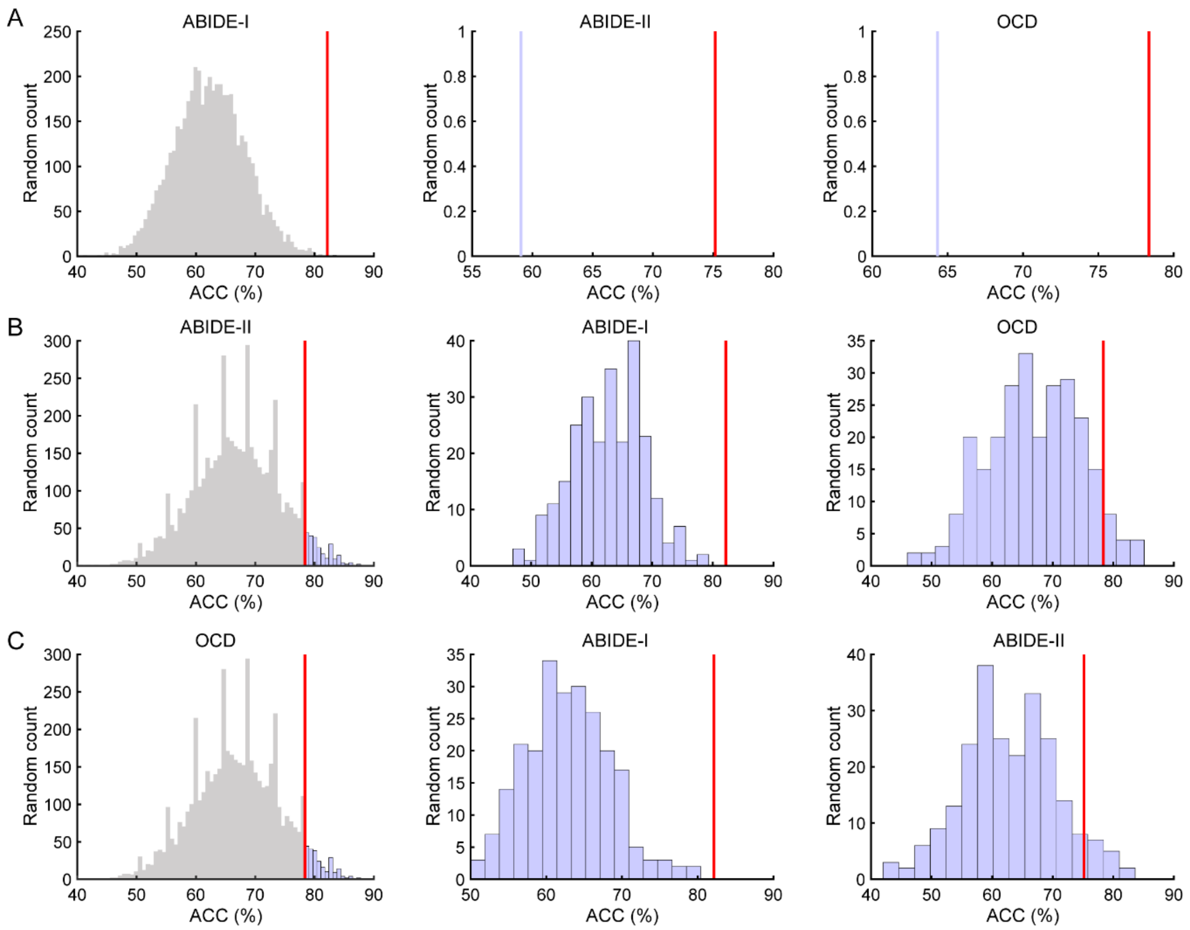

Figure S5. Plots depicting the poor generalizability of random selections of 9 core regions in different cohorts.

The left column shows the accuracy histograms of 9 core regions that were randomly selected 5,000 times in each dataset. Purple bars on the right side of the vertical red line denote cases with higher accuracy than the present monkey-derived classifier. Middle and right columns show the accuracy of these cases compared to the monkey-derived classifier in the other two datasets.

Supplementary Tables

Table S1. Characteristics of all TG and WT monkeys.

	ID	Gender	Copy number	Weight (kg)	Age (year)	Heart rate (beat/min)	$EtCO_2$ (mmHg)	Temp. (°C)	Isoflurane (%)	Run
TG	TG04	M	1.0	4.3	4.9	~115	~29	~37.0	1.0	9
	TG06	F	7.3	2.7	4.3	~103	~24	~35.6	1.0	8
	TG08	M	2.9	3.8	4.2	~125	~29	~36.1	1.0	7
	TG10	F	1.1	2.6	4.2	~94	~26	~35.8	1.0	8
	TG11	F	1.9	2.9	4.4	~130	~27	~36.8	1.2	13
		2M3F		3.26±0.75[a]	4.40±0.29[a]					45
WT	WT030	F	-	3.5	4.8	~148	~27	~37.7	0.8	8
	WT032	M	-	3.9	4.4	~120	~30	~37.7	1.0	10
	WT034	M	-	3.5	4.4	~120	~30	~37.0	1.0	7
	WT139	M	-	7	5.5	~148	~27	~37.2	1.2	10
	WT278	F	-	3.4	4.5	~125	~28	~35.6	1.2-1.25	10
	WT330	F	-	4.3	4.6	~125	~27	~35.9	1.2-1.3	10
	WT358	F	-	3.2	4.2	~130	~28	~37.8	1.25-1.3	10
	WT362	F	-	3	4.5	~130	~27	~36.1	1.2	10
	WT463	M	-	6.1	5.1	~110	~27	~37.2	1.3-1.2	5
	WT490	F	-	2.9	4.1	~136	~30	~37.1	1.1	9
	WTTT	F	-	2.9	5.4	~159	~27	~37.0	1.2	10
		4M7F		3.97±1.36[a]	4.68±0.46[a]					99
p-value		0.89 [b]			0.233 [c]					

Abbreviations. $EtCO_2$, end tidal of CO_2; Temp., rectal temperature; TG, transgenic; WT, wild-type.

[a], mean ± SD; [b], χ^2 test; [c], two sample student's t-test with two tails.

Table S2. Characteristics of human ABIDE-I cohorts.

Site	Number		Autism/Asperger/PDD-NOS	Age, mean±SD [Range]			Gender (M/F)			FIQ, mean±SD [Range]		
	HC	ASD		HC	ASD	p^a	HC	ASD	p^b	HC	ASD	p^a
KKI	21	5	1/4/0	10.10±1.15 [8.39 12.77]	9.87±1.52) [8.09 11.37]	.701	14/7	4/1	.562	113.14±9.54 [98.00 125.00]	98.60±15.29 [84.00 120.00]	.012
LEUVEN_1	14	13	13/0/0	23.36±3.00 [18.00 29.00]	21.77±4.27 [18.00 32.00]	.271	14/0	13/0	--	113.43±12.15 [98.00 146.00]	108.00±12.44 [89.00 128.00]	.262
MAX_MUN	24	12	0/12/0	25.92±8.32 [7.00 46.00]	32.08±14.46 [11.00 58.00]	.112	23/1	10/2	.201	112.13±9.78 [95.00 129.00]	114.67±12.62 [93.00 133.00]	.509
PITT	20	18	18/0/0	18.87±6.51 [11.81 33.24]	19.07±7.22 [11.40 33.86]	.928	17/3	14/4	.566	110.15±9.10 [97.00 130.00]	114.00±12.08 [96.00 131.00]	.272
SDSU	16	7	1/6/0	13.98±1.94 [8.67 16.88]	15.31±1.89 [12.13 17.15]	.143	10/6	7/0	.059	106.94±10.99 [88.00 123.00]	122.71±12.45 [112.00 141.00]	.006
TRINITY	23	19	7/6/6	17.48±3.66 [12.04 25.66]	16.63±3.02 [12.00 23.08]	.424	23/0	19/0	--	110.65±12.15 [89.00 133.00]	110.63±14.10 [89.00 135.00]	.996
UCLA_1	25	24	24/0/0	13.55±1.99 [9.50 17.79]	13.48±2.72 [8.49 17.94]	.914	21/4	22/2	.413	104.12±9.69 [84.00 126.00]	104.96±12.19 [86.00 132.00]	.791
UCLA_2	9	7	7/0/0	12.23±1.14 [9.79 13.63]	12.68±1.99 [10.57 16.47]	.576	7/2	7/0	.182	112.44±10.36 [99.00 128.00]	94.71±11.63 [86.00 118.00]	.006
UM_1	34	18	14/3/1	14.02±3.14 [9.50 19.20]	13.60±2.44 [9.70 18.60]	.621	22/12	13/5	.583	109.34±9.64 [89.00 127.50]	107.81±12.32 [89.50 135.00]	.623
UM_2	17	10	8/2/0	17.14±4.27 [13.60 28.80]	15.28±1.49 [13.10 17.40]	.198	16/1	9/1	.693	109.88±10.10 [89.50 129.00]	113.25±14.73 [90.50 133.50]	.487
Total	203	133	93/33/7	16.66±6.33 [7.00 46.00]	17.25±7.76 [8.09 8.09]	.447	167/36	118/15	.107	109.92±10.43 [84.00 146.00]	109.33±13.78 [84.00 141.00]	.655

Table S2 continued.

	ADOS, mean±SD [Range]			
Site	ADOS_TOTAL	ADOS_COMM	ADOS_SOCIAL	ADOS_STEREO
KKI	12.20±3.19 [8.00 16.00]	3.20±0.84 [2.00 4.00]	9.00±2.74 [6.00 13.00]	3.40±2.30 [0.00 6.00]
LEUVEN_1	--	--	--	--
MAX_MUN	--	--	--	--
PITT	12.50±3.71 [7.00 19.00]	4.19±1.33 [2.00 7.00]	8.31±2.73 [5.00 12.00]	2.08±1.55 [0.00 6.00]
SDSU	--	--	--	--
TRINITY	--	--	--	--
UCLA_1	10.42±4.21 [2.00 17.00]	3.25±1.65 [0.00 6.00]	7.17±2.87 [2.00 11.00]	1.33±1.69 [0.00 7.00]
UCLA_2	13.50±2.81 [9.00 16.00]	3.67±1.51 [1.00 5.00]	9.83±1.60 [8.00 12.00]	3.00±1.79 [1.00 6.00]
UM_1	--	--	--	--
UM_2	--	--	--	--
Total[c]	11.61±3.91 [2.00 19.00]	3.59±1.50 [0.00 7.00]	8.02±2.78 [2.00 13.00]	1.96±1.83 [0.00 7.00]

Abbreviations. TDC, typically developing control; ADOS, Autism Diagnostic Observation Schedule; ADOS_TOTAL, classic total ADOS score; ADOS_COMM, communication total sub-score of the classic ADOS; ADOS_SOCIAL, social total score of the classic ADOS; ADOS_STEREO, stereotyped behaviors and restricted interests total sub-score of the classic ADOS. KKI, Kennedy Krieger Institute; LEUVEN_1, University of Leuven: Sample 1; MAX_MUN, Ludwig Maximilians University Munich; PITT, University of Pittsburgh School of Medicine; SDSU, San Diego State University;

TRINITY, Trinity Centre for Health Sciences; UCLA_1, University of California Los Angeles: Sample 1; UCLA_2, University of California Los Angeles: Sample 2; UM_1, University of Michigan: Sample 1; UM_2, University of Michigan: Sample 2.

a, two sample Student's *t*-test with two tails; b, χ^2 test; c, 51 of 126 ASD subjects have ADOS_TOTAL, ADOS_COMM, ADOS_SOCAIL data available and 48 for ADOS_STRERO; "--" indicates data unavailable.

Table S3. Characteristics of human ABIDE-II cohorts.

Site	Number		Autism/Asperger/PDD-NOS	Age, mean±SD [Range]			Gender (M/F)			FIQ, mean±SD [Range]		
	HC	ASD		HC	ASD	p[a]	HC	ASD	p[b]	HC	ASD	p[a]
GU_1	39	23	9/12/2	10.49±1.74 [8.06 13.80]	11.29±1.05 [9.22 13.13]	.051	18/21	20/3	.001	121.08±14.05 [95.00 149.00]	117.61±13.98 [92.00 139.00]	.351
NYU_1	22	17	5/0/12	9.68±3.78) [5.90 23.81]	10.43±6.94 [5.43 34.76]	.669	20/2	16/1	.709	116.27±14.48 [91.00 144.00]	111.88±14.79 [87.00 138.00]	.358
TCD_1	18	12	3/9/0	16.28±2.79 [12.00 20.00]	14.75±3.54 [10.00 19.50]	.198	18/0	12/0	--	120.11±10.60 [99.00 142.00]	113.92±14.01 [83.00 139.00]	.179
UCLA_1	10	8	8/0/0	9.93±2.15 [7.76 14.09]	12.85±1.80 [9.66 15.03]	.007	6/4	8/0	.043	117.80±14.14 [94.00 141.00]	106.25±9.95 [93.00 118.00]	.069
Total	89	60	25/21/14	11.40±3.59 [5.90 23.81]	11.95±4.33 [5.43 5.43]	.402	62/27	56/4	.000	119.33±13.47 [91.00 149.00]	113.73±13.96 [83.00 139.00]	.016

Table S3 continued

Site	ADOS_G, mean±SD [Range]			
	ADOS_TOTAL	ADOS_COMM	ADOS_SOCIAL	ADOS_STEREO
GU_1	10.53±4.79 [3.00 18.00]	3.00±1.45 [1.00 7.00]	7.53±3.81 [2.00 14.00]	1.79±1.72 [0.00 5.00]
NYU_1	8.64±2.21 [5.00 12.00]	2.14±1.10 [1.00 4.00]	6.50±1.29 [4.00 8.00]	1.36±1.01 [0.00 4.00]
TCD_1	8.25±1.82 [7.00 12.00]	2.75±0.75 [2.00 4.00]	5.50±1.62 [3.00 8.00]	0.17±0.58 [0.00 2.00]
UCLA_1	13.00±0.71 [12.00 14.00]	3.80±0.84 [3.00 5.00]	9.20±0.45 [9.00 10.00]	3.20±1.64 [1.00 5.00]
Total[c]	9.70±3.56 [3.00 18.00]	2.78±1.23 [1.00 7.00]	6.92±2.75 [2.00 14.00]	1.42±1.55 [0.00 5.00]

Abbreviations. TDC, typically developing control; ADOS, Autism Diagnostic Observation Schedule; ADOS_TOTAL, classic total ADOS score; ADOS_COMM, communication total sub-score of the classic ADOS; ADOS_SOCIAL, social total score of the classic ADOS; ADOS_STEREO, stereotyped behaviors and restricted interests total sub-score of the classic ADOS. GU_1, Georgetown University; NYU_1, New York University Langone Medical Center: Sample 1; TCD_1, Trinity Centre for Health Sciences; UCLA_1, University of California Los Angeles.

a, two sample Student's *t*-test with two tails; b, χ^2 test; c, 48 of 60 ASD subjects have ADOS data available; "--" indicates data unavailable.

Table S4. Characteristics of human ADHD cohorts.

Site	Number		Age, mean±SD [Range]			Gender (M/F)			FIQ, mean±SD [Range]		
	HC	ADHD	HC	ADHD	p-value[a]	HC	ADHD	p-value[b]	HC	ADHD	p-value[a]
KKI	45	15	10.50±1.28 [8.12 12.87]	10.76±1.55 [8.10 12.99]	0.522	25/20	7/8	0.55	110.07±11.55 [85.00 134.00]	109.27±13.84 [88.00 134.00]	0.826
OHSU	25	18	9.27±1.22 [7.58 11.92]	9.09±1.15 [7.42 11.83]	0.633	13/12	13/5	0.181	119.64±13.18 [98.00 144.00]	107.00±13.88 [82.00 132.00]	0.004
Peking_1	57	20	11.12±1.61 [8.42 14.83]	11.35±2.35 [9.00 17.33]	0.627	16/41	16/4	0.000	118.23±13.85 [81.00 143.00]	97.85±12.40 [81.00 128.00]	0.000
Peking_2	22	27	11.53±1.85 [9.08 14.33]	12.69±1.76 [9.25 15.83]	0.030	22/0	27/0	--	121.45±13.68 [94.00 153.00]	111.37±12.89 [86.00 135.00]	0.011
Peking_3	21	16	13.24±0.99 [11.25 14.92]	13.40±1.33 [11.00 16.00]	0.680	21/0	16/0	--	113.14±13.05 [84.00 135.00]	102.06±10.42 [83.00 120.00]	0.009
Total	170	96	11.00±1.79 [7.58 14.92]	11.55±2.24 [7.42 17.33]	0.028	97/73	79/17	0.000	116.06±13.57 [81.00 153.00]	105.85±13.52 [81.00 135.00]	0.000

Abbreviations. TDC, typically developing control. KKI, Kennedy Krieger Institute; OHSU, Oregon Health & Science University; Peking, Peking University.

a, two sample Student's *t*-test with two tails; b, χ^2 test; "--" indicates data unavailable.

Table S5. Characteristics of human OCD cohorts.

Site	Number		Age, mean±SD [Range]			Gender (M/F)			OCD, mean±SD	
	HC	OCD	HC	OCD	p^a	HC	OCD	p^b	Y-BOCS	HAM-A
ION	58	78	30.79±8.41 [21.00 62.00]	31.04±8.94 [14.00 63.00]	.871	38/20	45/33	.355	30.12±6.77	17.92±10.27
Ruijin	21	14	30.81±5.84 [24.00 45.00]	27.29±10.87 [16.00 46.00]	.221	13/8	10/4	.561	24.29±5.50	15.50±9.67
Total	79	92	30.80±7.77 [21.00 62.00]	30.47±9.30 [14.00 14.00]	.803	51/28	55/37	.521	29.23±6.89	17.55±10.17

Abbreviations. OCD, Obsessive compulsive disorder; Y-BOCS, Yale-Brown Obsessive Compulsive Scale; HAM-A, Hamilton Anxiety Rating Scale.

a, two sample Student's *t*-test with two tails; b, χ^2 test.

Table S6. Imaging protocols for resting-state fMRI used in the present study.

ABIDE-I ASD cohort.

Parameter	Site									
	KKI	LEUVEN_1	MAX_MUN	PITT	SDSU	TRINITY	UCLA_1	UCLA_2	UM_1	UM_2
MRI Scanner	Philips Achieva	Philips	Siemens Magnetom Verio	Siemens Magnetom Allegra	GE MR750	Philips Achieva	Siemens Magnetom TrioTim	Siemens Magnetom TrioTim	GE Signa	GE Signa
Magnetic field strength (T)	3	3	3	3	3	3	3	3	3	3
Field of view (mm)	256	230	192	200	220	240	192	192	220	220
Matrix	84×81	64×64	--	64×64	64×64	80×80	64×64	64×64		
Number of slices	47	32	28	29		38	34	34	40	40
In-plane resolution (mm)	3.05×3.15	3.59×3.59	3.0×3.0	3.1×3.1	3.4×3.4	3.0×3.0	3.0×3.0	3.0×3.0	3.4×3.4	3.4×3.4
Slice thickness (mm)	3	4	4	4	3.4	3.5	4	4	3	3
Slice gap (mm)	0	0	--	0	0	0.35	0	0	0	0
TR (ms)	2500	1667	3000	1500	2000	2000	3000	3000	2000	2000
TE (ms)	30	33	30	25	30	28	28	28	30	30
Total scan time (mm:ss)	6:40	7:06	6:06	5:06	6:10	5:06	6:06	6:06	10:00	10:00
Flip angle	75	90	80	70	90	90	90	90	90	90
Slice acquisition order	Ascending	Ascending	--	Ascending	Ascending	Ascending	Ascending	Ascending	--	--
Eyes during scan	Opened	Opened	Closed/Opened	Closed	Opened	Closed	Opened	Opened	Opened	Opened

KKI, Kennedy Krieger Institute; LEUVEN_1, University of Leuven: Sample 1; MAX_MUN, Ludwig Maximilians University Munich; PITT, University of Pittsburgh School of Medicine; SDSU, San Diego State University; TRINITY, Trinity Centre for Health Sciences; UCLA_1, University of California Los Angeles: Sample 1; UCLA_2, University of California Los Angeles: Sample 2; UM_1, University of Michigan: Sample 1; UM_2, University of Michigan: Sample 2.

Table S6 continued.

ABIDE-II ASD cohort

Parameter	Site			
	GU_1	NYU_1	TCD_1	UCLA_1
MRI Scanner	Siemens Trio	Siemens Allegra	Philips Achieva	Siemens Magnetom TrioTim
Magnetic field strength (T)	3	3	3	3
Field of view (mm)	192	192	240	192
Matrix	64×64	64×64	80×80	64×64
Number of slices	43	33	37	34
In-plane resolution (mm)	3.0×3.0	3.0×3.0	3.0×3.0	3.0×3.0
Slice thickness (mm)	2.5	3	3.2	4
Slice gap (mm)	0.5	0	0.3	0
TR (ms)	2000	2000	2000	3000
TE (ms)	30	15	27	28
Total scan time (mm:ss)	5:14	6:00	7:06	6:06
Flip angle	90	82	90	90
Slice acquisition order	Ascending	Ascending	Ascending	Ascending
Eyes during scan	Opened	Opened	Opened	Opened

GU_1, Georgetown University; NYU_1, New York University Langone Medical Center: Sample 1; TCD_1, Trinity Centre for Health Sciences; UCLA_1, University of California Los Angeles.

ADHD cohort

Parameter	Site				
	KKI	OHSU	Peking_1	Peking_2	Peking_3
MRI Scanner	Siemens Trio	Siemens Magnetom TrioTim	Siemens Magnetom TrioTim	Siemens Magnetom TrioTim	Siemens Magnetom TrioTim
Magnetic field strength (T)	3	3	3	3	3
Field of view (mm)	256	240	200	200	200
Matrix	84×81	--	--	--	--
Number of slices	47	36	33	33	33
In-plane resolution (mm)	3.05×3.15	3.8×3.8	3.1×3.1	3.1×3.1	3.1×3.1
Slice thickness (mm)	3	3.8	3.5	3.5	3.5
Slice gap (mm)	0	--	--	--	--
TR (ms)	2500	2000	2000	2000	2000
TE (ms)	30	30	30	30	30
Total scan time (mm:ss)	6:40	3:32	8:06	8:06	8:06
Flip angle	75	90	90	90	90
Slice acquisition order	Ascending	Ascending	Ascending	Ascending	Ascending
Eyes during scan	Opened	Opened	Opened/Closed	Opened/Closed	Opened/Closed

KKI, Kennedy Krieger Institute; OHSU, Oregon Health & Science University; Peking, Peking University

Table S7. Cortical and subcortical parcellation and abbreviations.

Lobes	Number	Hemisphere	Number	Hemisphere	Abbreviation	Full name
Occipital	1	L	2	R	V1	Visual area 1 (primary visual cortex)
	3	L	4	R	V2	Visual area 2 (secondary visual cortex)
	5	L	6	R	VACv	Anterior visual area, ventral part
	7	L	8	R	VACd	Anterior visual area, dorsal part
Parietal	9	L	10	R	S1	Primary somatosensory cortex
	11	L	12	R	S2	Secondary somatosensory cortex
	13	L	14	R	mPC	Medial parietal cortex
	15	L	16	R	IPS	Intraparietal cortex
	17	L	18	R	IPL	Inferior parietal cortex
	19	L	20	R	SPL	Superior parietal cortex
Temporal	21	L	22	R	A1	Primary auditory cortex
	23	L	24	R	A2	Secondary auditory cortex
	25	L	26	R	TCpol	Temporal polar cortex
	27	L	28	R	IT	Inferior temporal cortex
	29	L	30	R	VTC	Ventral temporal cortex
	31	L	32	R	CTC	Central temporal cortex
	33	L	34	R	CTC	Superior temporal cortex
	35	L	36	R	HC	Hippocampus
	37	L	38	R	PHC	Parahippocampal cortex
PFC	39	L	40	R	M1	Primary motor cortex
	41	L	42	R	vlPMC	Ventrolateral premotor cortex
	43	L	44	R	dlPMC	Dorsolateral premotor cortex
	45	L	46	R	mPMC	Medial premotor cortex
	47	L	48	R	FEF	Frontal eye field
	49	L	50	R	vlPFC	Ventrolateral prefrontal cortex
	51	L	52	R	clPFC	Centrolateral prefrontal cortex
	53	L	54	R	dlPFC	Dorsolateral prefrontal cortex
	55	L	56	R	dmPFC	Dorsomedial prefrontal cortex
	57	L	58	R	mPFC	Medial prefrontal cortex
	59	L	60	R	PFCpol	Prefrontal polar cortex
OFC	61	L	62	R	iOFC	Orbitoinferior prefrontal cortex
	63	L	64	R	mOFC	Orbitomedial prefrontal cortex
	65	L	66	R	lOFC	Orbitolateral prefrontal cortex
Cingulate	67	L	68	R	sgACC	Subgenual cingulate cortex
	69	L	70	R	PCC	Posterior cingulate cortex
	71	L	72	R	rsCC	Retrosplenial cingulate cortex
	73	L	74	R	ACC	Anterior cingulate cortex
Insula	75	L	76	R	G	Gustatory cortex

	77	L	78	R	Ia	Anterior insula
	79	L	80	R	Ip	Posterior insula
Subcortical	81	L	82	R	Amyg	Amygdala
	83	L	84	R	Cau	Caudate
	85	L	86	R	Put	Putamen
	87	L	88	R	Tha	Thalamus
	89	L	90	R	HT	Hypothalamus
	91	L	92	R	NAcc	Nucleus accumbens
	93	L	94	R	GP	Globus pallidus

Table S8. Classification performance of classifiers based on different sets of core regions.

	Data set used to identify core regions	ACC (%) [95% CI]	Sensitivity (%) [95% CI]	Specificity (%) [95% CI]	AUC	*p*
ABIDE-I	Monkey	82.14 [77.53%, 86.00%]	79.70 [71.66%, 85.98%]	83.74 [77.78%, 88.40%]	0.884	<0.001
	ABIDE-II	61.31 [55.85%, 66.51%]	56.39 [47.53%, 64.88%]	64.53 [57.49%, 71.02%]	0.644	
ABIDE-II	Monkey	75.17 [67.30%, 81.71%]	70.00 [56.63, 80.80%]	78.65 [68.43%, 86.35%]	0.769	0.003
	ABIDE-I	60.40 [52.04%, 68.21%]	53.33 [40.10%, 66.14%]	65.17 [54.26%, 74.76%]	0.611	
OCD	Monkey	78.36 [71.29%, 84,13%]	73.91 [63.53%, 82.26%]	83.54 [73.14%, 90.61%]	0.848	--
	ABIDE-I	69.59 [62.02%, 76.26%]	63.04 [52.29%, 72.69%]	77.22 [66.15%, 85.59%]	0.790	0.044[a]
	ABIDE-II	60.23 [52.45%, 67.54%]	57.61 [46.87%, 67.71%]	63.29 [51.64%, 73.64%]	0.674	<0.001[b]
ADHD	Monkey	68.80 [62.80%, 74.24%]	56.25 [45.76%, 66.23%]	75.88 [62.80%,81.96 %]	0.700	--
	ABIDE-I	68.42 [62.41%, 73.89%]	61.46 [50.94%, 71.05%]	72.35 [64.88%, 78.79%]	0.754	0.920[a]
	ABIDE-II	62.03 [55.88%, 67.83%]	51.04 [40.69%, 61.31%]	68.24 [60.60%, 75.04%]	0.649	0.048[b]

Comparisons between different classifiers were conducted using McNemar's test. [a] denotes the monkey-derived classifier in comparison with the ABIDE-I derived classifier. [b] denotes the monkey-derived classifier in comparison with the ABIDE-II derived classifier.

ACC, accuracy; AUC, area under the receiver operating characteristic curve.

Table S9. Correlations between node strength and symptom severity in ASD and OCD cohorts.

Core region	ABIDE-II				OCD			
	ADOS TOTAL		ADOS COMM		Y-BOCS		HAM-A	
	r	*p*	*r*	*p*	*r*	*p*	*r*	*p*
CTC.L	-0.307	.034	-0.308	.033	-0.082	.44	-0.199	.058
STG.R	-0.278	.056	-0.336	.020	-0.050	.636	-0.209	.046
vlPFC.R	-0.282	.052	-0.333	.021	-0.217	.038	-0.209	.046
S1.R	-0.294	.043	-0.315	.029	-0.132	.208	-0.124	.237
M1.R	-0.284	.050	-0.264	.070	-0.114	.277	-0.166	.113
ACC.L	-0.219	.134	-0.295	.042	-0.085	.423	-0.091	.390
clPFC.R	-0.138	.351	-0.242	.098	-0.134	.204	-0.165	.117
SPL.L	-0.170	.249	-0.209	.153	-0.158	.132	-0.237	.023
dlPFC.R	-0.226	.123	-0.291	.045	-0.182	.083	-0.091	.387

CTC.L, left central temporal cortex; STG.R, right superior temporal cortex; vlPFC.R, right ventrolateral prefrontal cortex; S1.R, right primary somatosensory cortex; M1.R, right primary motor cortex; ACC.L, left anterior cingulate cortex; clPFC.R, right centrolateral prefrontal cortex; SPL.L, left superior parietal cortex; dlPFC.R, right dorsolateral prefrontal cortex. ADOS, Autism Diagnostic Observation Schedule; ADOS COMM, communication total sub-score of the classic ADOS; Y-BOCS, Yale-Brown Obsessive Compulsive Scale; HAM-A, Hamilton Anxiety Rating Scale.

Table S10. Prediction of symptom severity using functional connections identified in the classifier.

Data	Core region	Predicted model	r^2	r	p
ABIDE-II	STG.R	$ADOS\ COMM = 3.84 - 1.64 \times (STG.R{\sim}lOFC.R)$	0.166	0.407	0.004*
	vlPFC.R	$ADOS\ COMM = 3.96 - 2.06 \times (vlPFC.R{\sim}THa.R)$	0.191	0.437	0.002*
	S1.R	$ADOS\ COMM = 3.21 - 1.51 \times (S1.R{\sim}dmPFC.L)$	0.164	0.405	0.004*
	ACC.L	$ADOS\ COMM = 3.68 - 2.62 \times (ACC.L{\sim}STG.L) + 1.72 \times (ACC.L{\sim}mPC.L)$	0.226	0.475	<0.001*
	dlPFC.R	$ADOS\ COMM = 4.12 - 1.77 \times (dlPFC.R{\sim}STG.L)$	0.171	0.413	0.004*
OCD	vlPFC.R	$Y-BOCS = 31.86 - 5.07 \times (vlPFC.R{\sim}PFCpol.R)$	0.048	0.219	0.036*
	SPL.L	$HAM-A = 23.19 - 9.06 \times (SPL.L{\sim}CTC.L)$	0.079	0.281	0.007*

CTC.L, left central temporal cortex; STG.R, right superior temporal cortex; vlPFC.R, right ventrolateral prefrontal cortex; S1.R, right primary somatosensory cortex; ACC.L, left anterior cingulate cortex; dmPFC.L, left dorsomedial prefrontal cortex; SPL.L, left superior parietal cortex; dlPFC.R, right dorsolateral prefrontal cortex; mPC.L, left medial parietal cortex; IOFC.R, right lateral orbitofrontal cortex; THa.R, right thalamus; PFCpol.R, right prefrontal polar cortex. * indicates $p < 0.05$, FDR corrected.